SLAC–PUB–3063
February 1983
(I)

Investigation of Electrical Properties of a 120cm PSC Using an Inner Spark Pulser*

N. FUJIWARA,[a] A. OGAWA,
YU. PESTOV[b] AND R. SUGAHARA[c]

Stanford Linear Accelerator Center
Stanford University, Stanford, California 94305

Abstract

Characteristics of fast pulse propagation in a large planar spark counter (PSC) are simulated using a pulser located inside the spark gap. Besides the main mode of pulse propagation, three undesirable modes are observed. These latter strongly distort the shape of the pulse. Characteristics of these modes and methods to eliminate their effects are demonstrated. We present an electrical design for a 120cm spark counter along with some of its electrical properties as revealed by measurements made with the inner spark pulser. In the present counter design the charge of a pulse is shared by several neighboring strips, enabling one to measure the transverse position of a spark to a high degree of accuracy.

Submitted to Nuclear Instruments and Methods

* Work supported by the Department of Energy under DE-AC03-76SF00515 and the Japan-US Co-operative Research Project on High Energy Physics under the Japanese Ministry of Education, Science and Culture and the US Department of Energy.

[a] Present address: Department of Physics, Nara Women's University, Nara 630, Japan

[b] Present address: Academy of Science of the USSR, Siberian Division, Institute of Nuclear Physics, 630090 Novosibirsk, USSR

[c] Present address: National Laboratory for High Energy Physics, Oho-Machi, Tsukuba-Gun, Ibaraki-Ken, 305 Japan

1. Introduction

During the last several years Planar Spark Counters (PSC's) have been investigated extensively in order to improve the resolution of time of flight measurements for particle identification[1]. A time resolution of 25 ps has been obtained for a small counter of about 10 $cm \times 10\,cm$[2].

In a large PSC the transmission line properties of the counter are very important. Proper attention must be paid to this attribute in order to obtain good timing information from a counter. Characteristics of fast pulse propagation in a large PSC of 120 $cm \times 10\,cm$ size were measured with aid of a new device called an Inner Spark Pulser (ISP) and are discussed. A final electrical design for the PSC is presented along with several measured properties including pulse charge sharing between strips, strip-to-strip uniformity of pulse propagation velocity as well as transverse and longitudinal position resolution.

2. Inner Spark Pulser

To investigate the electrical properties of a large PSC, a device was constructed which simulates its function. In this section, the construction and characteristics of this device, called an ISP, are described.

In normal PSC operation, a spark, once initiated, will sustain itself until the (local) electric field in the gap is discharged. The semiconducting anode automatically quenches the spark, and only a small local area of the anode is discharged. Another spark cannot occur in this area until the local field strength in the gap recovers above some threshold value. Thus, if a sharp point is present in the gap, cyclic, anode-directed sparks should occur between the point and the anode in the manner of a relaxation oscillator. This is the basis of operation of the ISP.

Figure 1 shows the construction of such a device. A high (negative) potential is placed on the cathode, with the striplines at ground potential. Thus a high electric field exists at the tip of the needle and eventually a spark will jump between it and the copper anode affixed to the bottom of the glass with conductive adhesive. The semiconducting glass was 6.5 mm thick and had resistivity $\rho = 550\,G\Omega cm$. The spark gap was air. The copper anode was used in order to assure the stability of the spark pulse height. As is explained later, the voltage between the copper anode and the pulser point will never exceed threshold. However, the remainder of the gap is at full voltage. To prevent unwanted discharges, the cathode was insulated with mylar tape[3] everywhere but in the vicinity of the point of the needle.

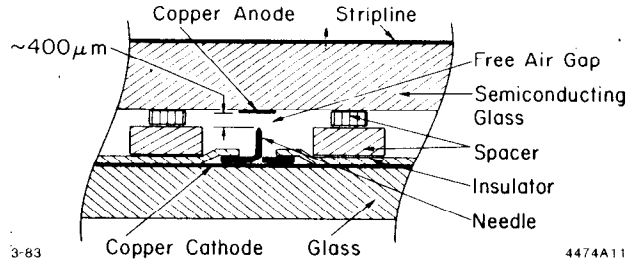

Figure 1. Construction detail of the Inner Spark Pulser(ISP), showing copper cathode covered with insulator, with attached needle pointed at the copper anode. Air gap spacing of $\sim 400\,\mu m$ is fixed by spacers. The semiconducting glass acts as a D.C. coupling between copper anode and ground, as well as the dielectric of a strip transmission line.

Typical pulse shape and pulse height distribution are shown in fig. 2. The pulse is roughly Gaussian in shape with a height of $10\,V$ and a FWHM of $1\,ns$. The rise time, measured with a sampling oscilloscope, was $300\,ps$. The width/mean of the pulse height distribution is 10%.

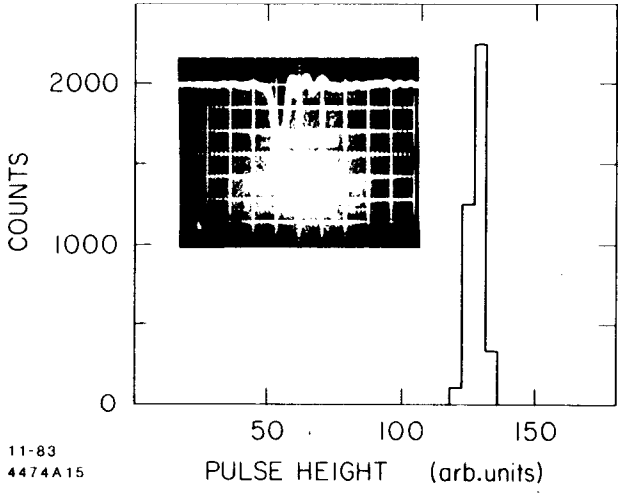

Figure 2. Inner spark pulser pulse height distribution. The width/mean is 10%. Inset: Typical pulse shape at $2\,V/div$ and $2\,ns/div$. The pulse has a Gaussian shape with a FWHM of $1ns$ and a rise time of $300\,ps$.

A plot of repetition rate versus applied voltage appears in fig. 3a. The pulse rate increases linearly with the applied voltage. This indicates that the spark occurs at a threshold voltage independent of the applied voltage, *i.e.* the ISP is a relaxation oscillator. From the slope of the curve on the figure and the inferred threshold voltage of $1\,kV$ we calculate the time constant of the oscillator to be $\tau = 1\,s$. This should also be the time constant of the effective RC network represented by the copper anode charging up through the semiconducting glass and capacitively coupled to the cathode. This is $\sim \rho\epsilon_0\kappa(1 + \frac{\delta/\kappa}{d})$ where δ is the thickness of the semiconducting glass, d is the distance from the copper anode to the cathode, ϵ_0 is the dielectric permittivity of space and κ is the dielectric constant of the glass. This quantity is $.64\,s$, in good agreement with the above time constant.

Figure 3b shows the dependence of the pulse amplitude on the area of the copper anode. The total charge induced on the striplines will be the charge on the copper anode at the moment the spark occurs. This will be $\sim V_\theta \frac{A}{d\epsilon_0}$ where V_θ is the threshold voltage and A is the area of the copper anode. For an anode area of $20\,mm^2$ this quantity is $200\,pC$. The pulse observed in this case has a peak height of $10\,V$ into $50\,\Omega$ and a width of $1\,ns$, which is in agreement with the hypothesis.

We observe that when the copper anode area is less than $10\,mm^2$ the pulse shape and amplitude are no longer stable. The rise time of the pulse also appears to be influenced by the area of the copper anode: as the area was increased, the rise time was seen to decrease somewhat.

The very stable performance of the inner spark pulser indicates that it may be employed as a reliable probe of the response of the PSC to a spark. In addition, the $1\,ns$ width of the pulse is an unexpected boon since it affords an even more stringent probe into the high frequency characteristics of the counters.

3. Pulse Propagation Modes and their Characteristics

In the $120\,cm$ long PSC the striplines of the counter are $10\,ns$ "long", twice as long as the $5\,ns$ width of pulses due to crossing of charged particles. In this case these transmission lines affect the pulse shape significantly.

The velocity of pulse propagation in a transmission line is a function of dielectric constant ϵ of the materials around the conductors. In the PSC, a semiconductor of high dielectric constant ($\epsilon \sim 10$) is used between anode strips and the cathode. Elsewhere the dielectric consists of gases or other materials of low dielectric constant.

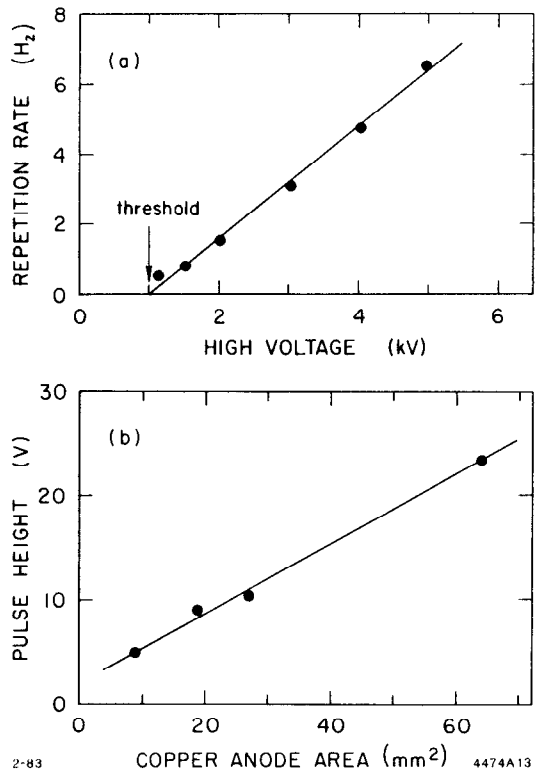

Figure 3. Inner spark pulser operating parameters. a) Repetition rate as a function of applied voltage. As in a relaxation oscillator, the pulse rate increases linearly with voltage. The threshold voltage is $\sim 1\,kV$ and the observed slope is consistent with the measured properties of the glass. b) Peak pulse height as a function of the area of the copper anode. Below an area of $20\,mm^2$ the pulse is not stable.

The mutual coupling of strips is strong in comparison with a device like a multi-wire proportional chamber. Therefore the propagation of pulses can be complex. In the present simulation, several modes of pulse propagation are observed. Characteristics of each mode and methods for abating the undesired ones are described in this section.

The structure of the test PSC of $120\,cm$ length and $10\,cm$ width is shown in fig. 4. It is very similar in form to an actual, operating PSC. An ISP was located in the air gap between the semiconducting glass and the cathode. The gap between the copper anode and the tip of the needle was about $400\,\mu m$. As in the case of the inner spark pulser described above, the resistivity of the semiconducting glass was $550\,G\Omega cm$ and its thickness was $6.5\,mm$. Eight striplines are arranged over the semiconductor. The width of the strip (W) was selected to be $10\,mm$ or $5\,mm$. The separation distance between strips (D) is from $1\,mm$ to $10\,mm$. Each end of each stripline was terminated in $50\,\Omega$. The repetition rate of the inner spark pulser was about $10\,Hz$. The pulse height on the strip just over the spark was about $10\,V$ and the pulse width was $1\,ns$.

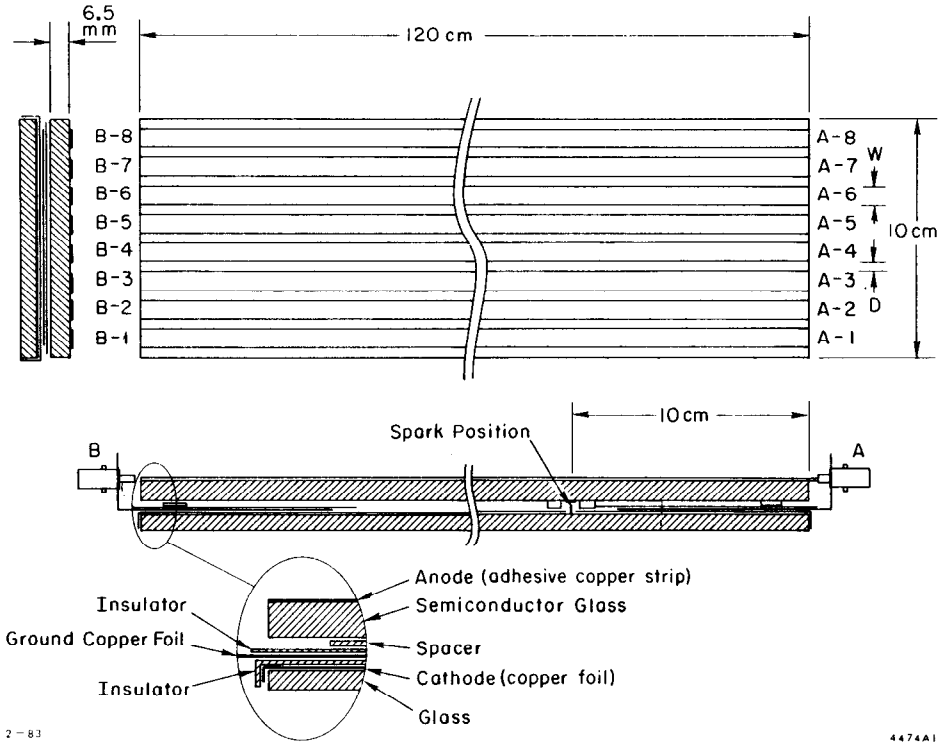

Figure 4. Schematic view of a test PSC of $120\,cm$ length. The ISP of fig. 1 was installed in the gap. The semiconducting glass had a resistivity of $550\,G\Omega cm$ and a thickness of $6.5\,mm$. The eight striplines on its upper surface had a width W of 5 or $10\,mm$ and separation D of 10 or $1\,mm$, respectively. Signals were coupled out at the two ends of the striplines, labeled A and B, on coaxial connectors.

3.1 Mode 1

The main mode of pulse propagation occurs between an anode strip and the cathode plate as depicted by the solid lines in fig. 5. This is the desired mode of pulse propagation. In the following, we discuss three additional modes of pulse propagation observed in this device, their properties and what means we employed to abate them. Table 1 presents a summary of this discussion.

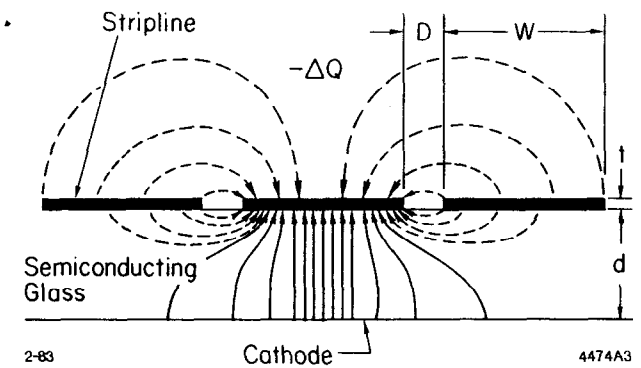

Figure 5. Electric field of pulses propagating along the length of a counter with three strips. Direction of propagation is perpendicular to the plane of the paper. Electric field lines of mode 1 are solid lines and those of mode 2 are dashed lines. Dimensions W and D are as in fig. 4. while δ is the thickness of the semiconducting glass, and d is the spark gap dimension.

3.2 Mode 2

Besides the main mode, a second mode of pulse propagation is observed. The distinctive feature of this mode is that the velocity of pulse propagation is faster than that of mode 1. Typical pulses obtained with three strips of $W = 10\,mm$ and $D = 1\,mm$ are shown in fig. 6a. The pulses were obtained from the strip centered over the spark. All strips were, of course, terminated in their characteristic impedence. The upper trace was obtained at end A in fig. 4 (near the spark) and the lower trace at end B (far from the spark). Two pulses are observed at end B. The earlier pulse is the second mode. The mode 1 pulse arrives $2\,ns$ later. The velocity of the mode 2 pulse is measured to be 1.3 times that of the mode 1 pulse under these conditions. As the upper trace shows, we cannot resolve the two modes at end A.

Table 1. Modes of pulse propagation in the PSC and their characteristics. Mode 1) the desired mode: balanced currents in stripline and cathode. Terminated in 50 Ω. Velocity determined by semiconducting glass. Mode 2) balanced pair pulse propagation. Neighboring strips have opposite charges and currents. Pulse velocity is critically dependent on ϵ of material covering the strips. Mode 3) all strips coupled together by magnetic component of field. This mode is reduced by eliminating the flux return path. Mode 4) parallel plate transmission line comprised of cathode and upper ground plane. This mode is eliminated in the same way as for mode 3.

	Mode 1	Mode 2	Mode 3	Mode 4
Field	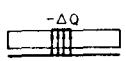		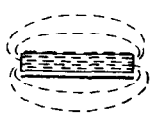	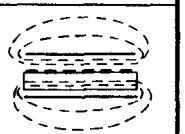
Mode	simple stripline mode	balanced currents in neighboring strips	common mode of all strips	cathode and upper ground plane transmission line
Pulse Shape				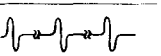
Amplitude	100%	~ 50%	~ 10%	~ 10%
Distinctive Features	velocity: $11\,cm/ns$	velocity: $14\,cm/ns$	same amplitude on every strip	damped oscillation
Method of Solution		matched dielectric constant 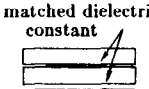	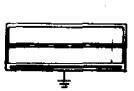	

12-83 4474A7

The amplitude and the velocity difference referred to above depend on strip separation D and the dielectric constant of the material over the strips. The velocity difference decreases as D increases. If we have only one strip, the second mode is not observed at all. Furthermore, if the dielectric constant of the material over the strips is identical to that of the anode, the velocity difference is small. Figure 6b shows the pulses when the strips are covered with material of the same dielectric constant as the anode $6.5\,mm$ thick, *i.e.* another piece of semiconducting glass. In this case, too, the two modes cannot be resolved.

Our understanding of the second mode is as follows: The broken lines in fig. 5 show the electric field lines for this mode. It constitutes a mode

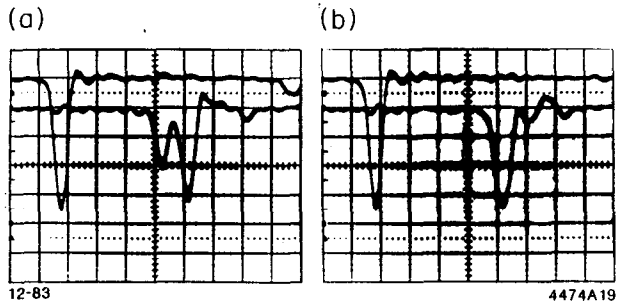

Figure 6. Oscilloscope traces of ISP pulses illustrating mode 2 phenomena. Scales are: $2\,ns/div$ and $2\,V/div$. Upper trace is $A-4$ (near end), lower trace is $B-4$ (far end). a) Without strip cover. The earlier of the two pulses in the lower trace is the spurious, mode 2 pulse. The mode 2 pulse is not discernible in the upper trace. b) With strip cover. The shape of the far end pulse is greatly improved.

of pulse transmission wherein two neighboring strips have balanced currents. The greater portion of the field is concentrated around the gap between strips. Without a strip cover, the effective dielectric constant "seen" by this mode is strongly affected by the relatively low ϵ of the air above the strips. In order to make the velocity of mode 2 be the same as that of mode 1, it is sufficient to cover the strips with a material of the same dielectric constant as the anode. The thickness of the strips t is made to be as small ($\leq 100\,\mu m$) as possible to avoid the presence of a gas gap between strips, especially important in the case of small D ($\sim 1\,mm$).

3.3 Mode 3

When the semiconducting glass is prepared with many strips as shown in fig. 4, the third mode of pulse propagation is observed. Typical features of this mode are:

- The pulses all have the same timing: They are created simultaneously and travel at the same velocity.
- The amplitude of this mode is approximately the same on every strip.
- The amplitude is about 10% of that of the mode 1 pulse observed on the strip centered over the spark.
- The pulse shape is a time-differentiated form of the mode 1 pulse.

Figure 7 shows pulses obtained with the strip configuration of fig. 4 with $W = 5\,mm$ and $D = 6\,mm$. Using a strip cover 6.5 mm thick of semiconducting glass eliminated mode 2, allowing us to study mode 3 alone. The spark position was just between strip 4 and strip 5 in fig. 4. The upper traces in fig. 7 were obtained at $A-4$ in fig. 4. The lower trace in fig. 7a was obtained at $B-8$ and represents mode 3 only. Normalized to the amplitude of the mode 1 pulse seen at $A-4$, the amplitude at $B-8$ is 8% and the amplitude at $A-8$ is 2% .

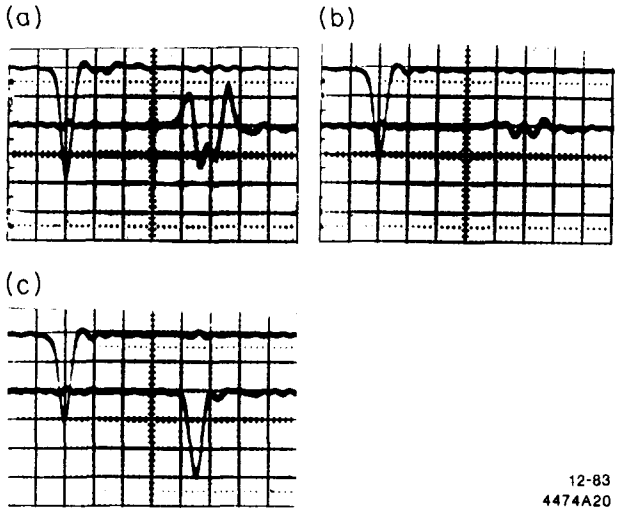

Figure 7. Oscilloscope traces showing mode 3 phenomena. Stripline dimensions were $W = 5\,mm$ and $D = 6\,mm$, respectively, and a strip cover with $\epsilon = 10$ abated mode 2. Time scale is $2\,ns/div$ for all traces. Upper trace is $A-4$(near end) at $2\,V/div$ in each case. a) Without the side shield in place. Lower trace is $B-8$(far end) at $0.5\,V/div$. This spurious pulse has the shape of the time differentiation of the mode 1 pulse, and about 8% the size. b,c) With the side shield in place, as in table 1. The lower trace in b) is from $B-8$ at $0.5\,V/div$, as in a): its amplitude is now smaller by a factor of 5. The lower trace in c) is from $B-4$ at $2\,V/div$, as in fig. 6. Its shape has been still further improved.

We note by comparison that, for the configuration with $W = 10\,mm$ and $D = 1\,mm$, the normalized amplitude at $B-8$ is 20% . Thus, as the strips get closer together, the amplitude of the third mode increases.

This mode is understood as follows: It constitutes a common mode of pulse propagation, in which the strips all carry equal currents. The magnetic field of the ensemble is shown in the third column of table 1. It envelopes all of the

strips and the cathode plane. This mode is eliminated by a copper foil ground surrounding the cathode plane and extending up beside the anode strips. This enclosing conductor prevents the magnetic field from reaching outside the lower dielectric.

Figure 7b,c shows signals obtained with this copper shield in place. The signal at $B-8$ appears as the lower trace of fig. 7b. The third mode is completely eliminated. The lower trace of fig. 7c shows the pulse obtained at $B-4$ in fig. 4. The pulse is very clean and its shape is close to that of the pulse obtained at $A-4$ (the upper trace). Referring to fig. 6b, lower trace, the pulse is not as large as that of the upper trace (some effect of mode 3 can be seen). These effects are both eliminated in fig. 7c.

3.4 Mode 4

The last mode is a damped oscillation of time constant *ca.* $100\,ns$ which was observed when the strips were covered with a conductor grounded at the two ends of the striplines but which did not extend down the sides. The arrangement of conductors can be seen in the fourth column of table 1. This mode was observed on every strip at both ends with the same amplitude.

Typical oscillograms are shown in fig. 8a obtained under the same conditions as the case of fig. 7a, except with a ground plane of copper foil over the counter, as described above. The time scale is $20\,ns/div$. The upper trace in the figure was obtained at $A-4$ in fig. 4. The main mode signal is off scale in this figure. The lower trace was obtained at $A-8$. The waveform appears to be that of a single pulse making multiple traverses of the counter, damping only a little bit with each cycle. The amptitude of the first pulse of the damped oscillation is $\sim 8\%$ of the amplitude of the mode 1 pulse at $A-4$.

This mode is significant in that any threshold-type electronics attached to a strip will be triggered repeatedly until the pulse damps down. Since these pulses appear on all strips, just one spark in the counter will "deaden" the entire counter for many hundreds of nanoseconds.

This mode is closely related to mode 3. The upper foil is one conductor of a parallel plate transmission line, the other being the cathode plate. This transmission line is shorted at both ends and the pulse on this line is completely reflected with inverted polarity at each end of the counter. The cycle time of this oscillation just corresponds to the electrical length of the counter. The oscillating pulses induce pulses on each strip electrostatically.

This mode is removed by the same method as for mode 3, namely by using a grounding conductor around the entire counter. Figure 8b shows the

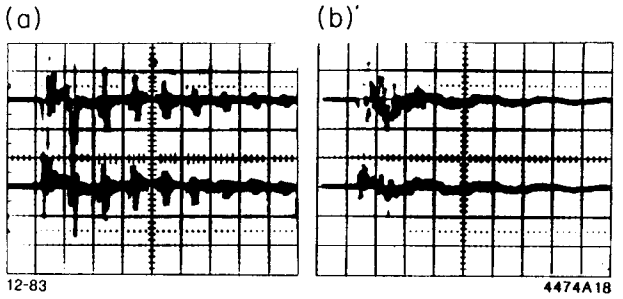

Figure 8. Oscilloscope traces illustrating mode 4 phenomena. Conditions were the same as for fig. 7. Scales of all traces are $0.2\,V/div$ and $20\,ns/div$. Upper trace: $A-4$, lower trace: $A-8$. a) Ground plane as in top line of table 1. b) Ground plane as in bottom line of table 1.

same signals as fig. 8a but employing upper and lower conductive foil shields connected along the sides of the counter. Mode 4 oscillations are now greatly reduced.

3.5 Summary

The above four modes are summarized in table 1. The shape of the mode 1 pulse is strongly modulated by the other modes. Therefore, to obtain good time- and position resolution, it is very important that the effects of the undesired modes be completely removed. Any apparatus of large size utilizing fast-rise pulses and many channels should be carefully designed taking these concepts into account.

4. Electrical Design for a $120\,cm$ *PSC* and its Performance

An electrical design for a long *PSC* based on the above results is shown in fig. 9. A material with $\epsilon = 10$ and thickness $6.7\,mm$ was used as a strip cover[4]. For this design, $W = 5\,mm$ and $D = 6\,mm$, and the characteristic impedance for mode 1 was $50\,\Omega$.

4.1 Pulse Shape and Suppression of Unwanted Modes

Pulses obtained from some of the strips are shown in fig. 10. The inner spark pulser was located directly under strip 4. The desired pulse shape was obtained for each strip.

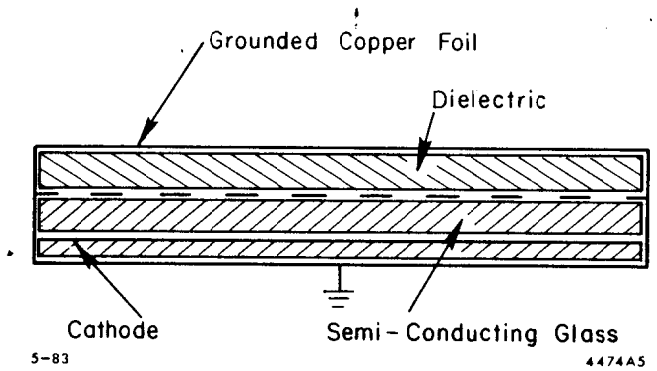

Figure 9. Electrical design for long PSC based on results of work with Inner Spark Pulser. Dielectric material with the same dielectric constant, $\kappa = 10$, as the semiconducting glass occupies the space above the striplines. With a strip width of $W = 10\,mm$, the striplines have a $50\,\Omega$ impedence. The strip separation was $D = 6\,mm$. Grounded striplines run along the edge of the assembly, and grounded copper foil completely surrounds all conductors.

4.2 Velocity of Pulse Propogation

Figure 11 shows the velocity of pulse propagation for the strips. Field compensating strips were arranged along the edge of the semiconducting glass as shown in fig. 9. These strips compensate the field near the edge of the counter so that the pulse velocity here will be as similar as possible to that of the other strips.

5. Position Resolution

The inner spark pulser was also used to investigate the ability of the PSC to measure the position of the spark in directions both longitudinal and transverse to the strips.

5.1 Longitudinal Position resolution

In our test setup we measured t_A and t_B, the arrival times of the pulses at the respective ends of the striplines. The mean time difference $\Delta t/2 = (t_A - t_B)/2$ was related to the longitudinal position of the spark y by the formula: $y = v(t_A - t_B)/2$, where v was the velocity of pulse propagation along the stripline. Using a device with two ISP's separated by $87\,mm$, we recorded $\Delta t/2$ for sparks from each of the ISP's. The data appear in fig. 12. We thus measured

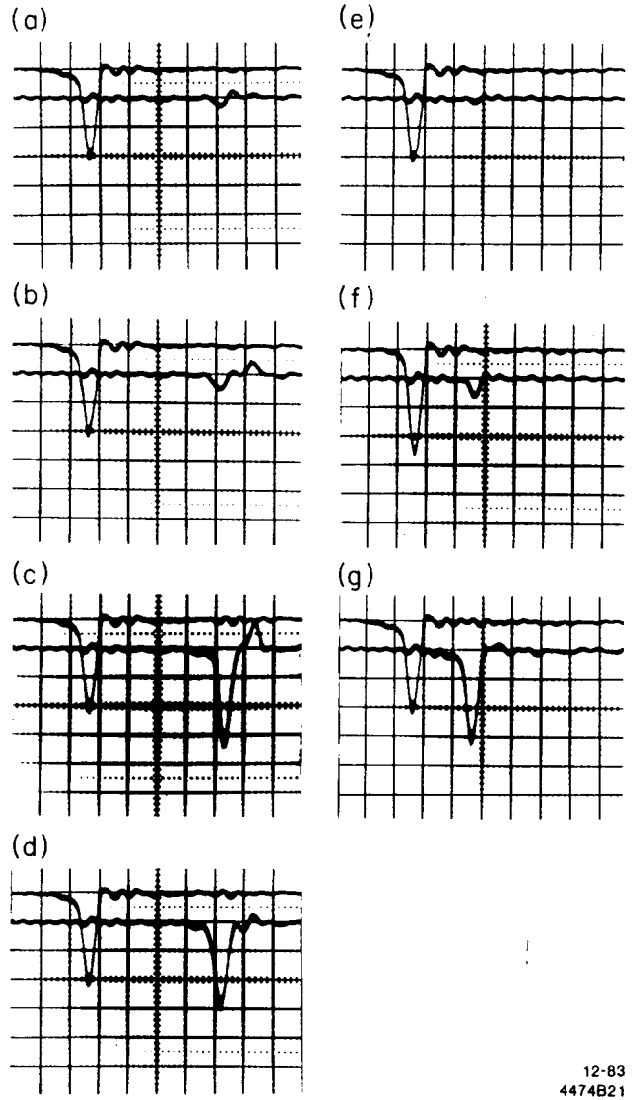

Figure 10. Pulse shapes for the strips for the configuration of fig. 9. Scales of all traces are $2\,V/div$ and $2\,ns/div$. Upper trace: $A-4$ (displaced from lower trace by $4\,ns$), lower trace: a) $B-1$, b) $B-2$, c) $B-3$, d) $B-4$, e) $A-1$, f) $A-2$, g) $A-3$.

v to be $87\,mm/600\,ps = 14\,cm/\,ns$, or $\beta = 0.5$. In these measurements the time bin of the digitizing electronics[5] was $25\,ps$. The observed resolution in y, $\sigma_y = .5\,mm$ was consistent with having arisen entirely from the TDC time bin.

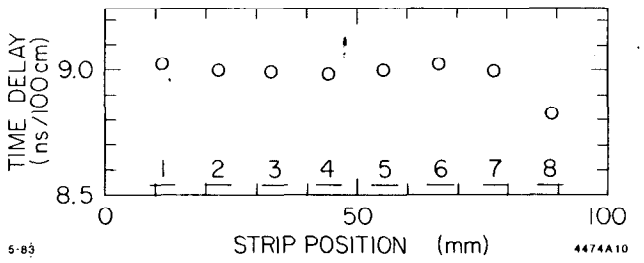

Figure 11. Transit time for each strip, measured with the *ISP*. Strip 8 deviates from the most probable value by 2%.

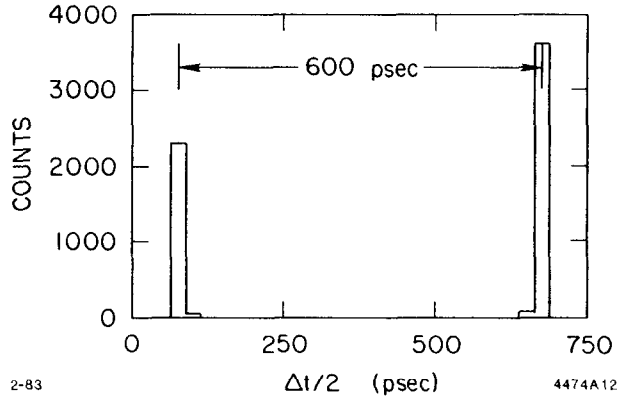

Figure 12. Mean time difference of pulse propagation $\Delta t/2 = (t_A - t_B)/2$ for two needles separated by $\Delta y = 87\,mm$. Velocity of pulse transmission $v = \frac{\Delta y}{\Delta t/2} = 14\,cm/\,ns$.

5.2 *Transverse Position resolution*

A spark in the *PSC* will induce a pulse of varying charge on all nearby strips. With this amount of pulse height sharing between strips, one can consider reading out the position using a method similar to that employed in cathode strip readouts in proportional chambers.

To make the following measurements, the *ISP* was installed in the inverted position. The point of the needle was thus directed toward the cathode. There was only one copper anode present: the base of the needle ($10\,mm \times 2\,mm$), which was in contact with the semiconducting glass. The position of the pulser was read out by means of a dial indicator in increments of $25.4\,\mu m$ ($0.001\,in$), with an uncertainty of $13\,\mu m$ ($0.0005\,in$).

Figure 13 shows the relative charge induced on a strip as a function of the

distance from the strip to the spark, obtained for the cases of $W = 5\,mm, D = 6\,mm$ and $W = 11\,mm, D = 1\,mm$. The proportion of the charge induced on each strip depends on the geometric dimensions of the counter, consistent with simply the solid angle subtended by the strip relative to the spark. For the following measurements, we had $W = 5\,mm, D = 6\,mm$. With the spark located directly below the center of a strip, all but 25% of the charge will be induced on that strip. If the spark is centered between two strips, together they will hold all but 6% of the charge. This charge-sharing profile indicates that the centroid of charge, $\mu = \sum_i x_i q_i / \sum_i q_i$, will be a good estimator of the spark position.

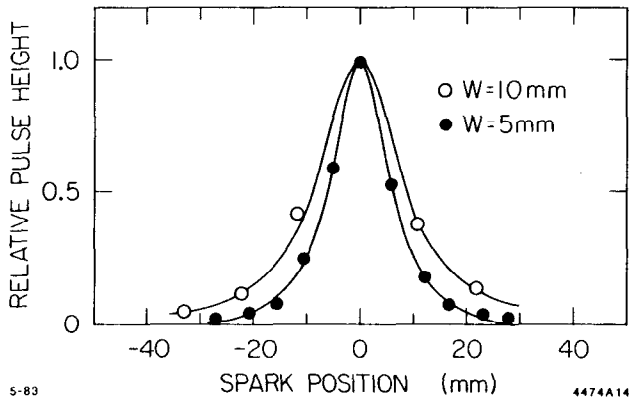

Figure 13. Sharing of the spark charge between strips. Relative pulse height induced in a strip as a function of the distance from the strip to the spark. The open circles are for an interstrip spacing of $W = 10\,mm$ and the closed circles are for $W = 5\,mm$.

Figure 14a shows the charge centroid as a function of the actual position x of the spark. These data cover a minute range, corresponding to half the interstrip spacing, or $\sim 6\,mm$. Over the range covered, these data may be approximated by a function of the form: $\mu = (.917)x + (-.304)\sin\theta + (.029)\sin 3\theta$, where μ and x are in units of mm, and $\theta = 2\pi x/11.6$. This function is the smooth curve in the figure. The fact that the multiplier of x in the formula is not exactly 1 arises from the discrepancy between the nominal strip spacing of $11\,mm$ and the actual spacing, as well as from the difference in the true widths of the strips. The appearance of $\sin\theta$ and $\sin 3\theta$ terms is due to the difference between the profile of fig. 13 and an ideal triangular distribution.

Figure 14b shows the difference between the data and the function. The

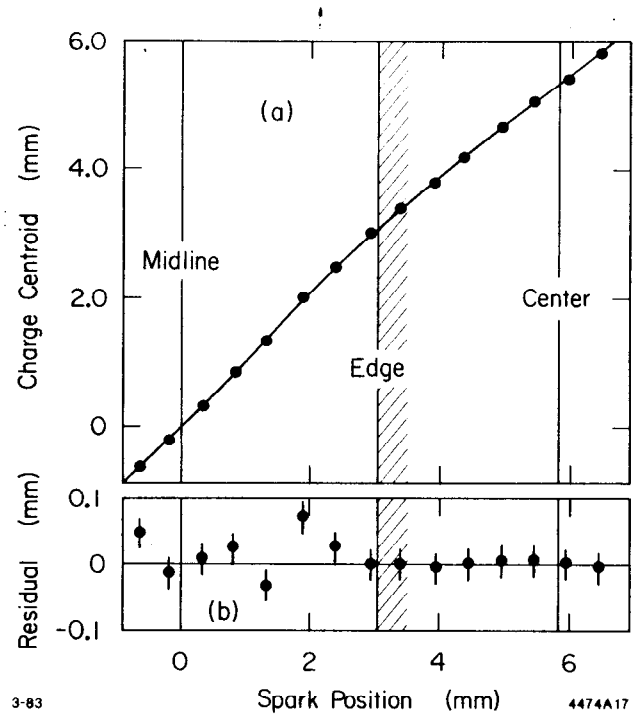

Figure 14. Charge centroid as a function of spark position. a) plot of $\mu = \sum_i x_i q_i / \sum_i q_i$ *vs.* spark position. "Midline" corresponds to the position midway between strips 4 and 5. "Center" marks the center of strip 4. The smooth curve is $\mu = (.917)x + (-.304)\sin\theta + (.029)\sin 3\theta$, where $\theta = 2\pi x/11.6$. b) residual of data (*i.e.* smooth curve subtracted off). The error bars reflect the variance of the data, not its uncertainty.

error bars represent the variance of the quantity μ rather than the standard deviation. A great deal of the scatter in the residual is due to inaccuracies in measuring x.

Figure 15 shows the distribution of μ for the spark pulser in the normal, upright position located directly below strip 4. In these circumstances, fluctuations in μ are dominated by fluctuations in the pulse heights of strips 3 and 5, representing only 25% of the total charge read out. The variance of this distribution is $\sim 24\,\mu m$, which amounts to $\sim 1/500$ of the interstrip spacing of $11\,mm$.

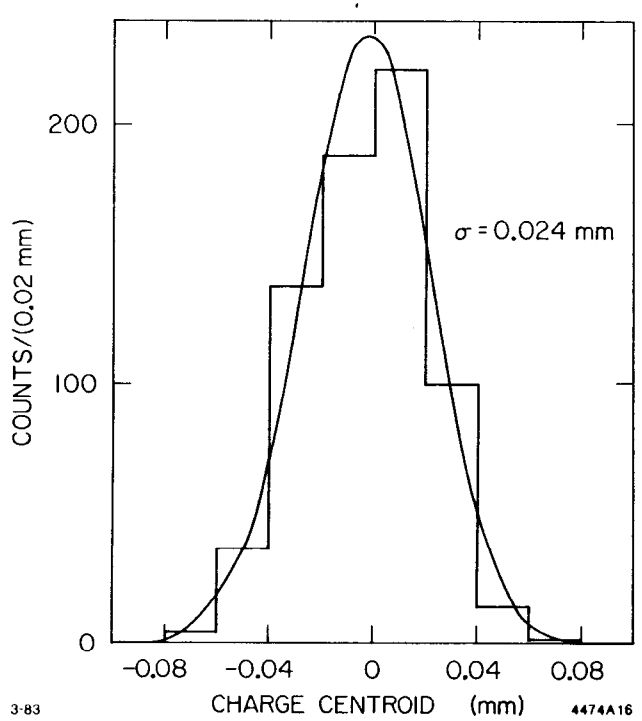

Figure 15. Distribution of μ with ISP in upright position, positioned directly below the center of strip 4. Fluctuations in μ are dominated by fluctuations in the small pulse heights of strips 3 and 5. Variance of distribution is $24\,\mu m$. This corresponds to $\sim 1/500$ the interstrip spacing of $11\,mm$.

6. Conclusions

We have reported on the development of a new device to create pulses inside the planar spark counter in order to probe its electrical properties. The fine attributes of the inner spark pulser have enabled us to readily solve several thorny problems as concerns pulse propagation in the PSC, as well as measure such things as pulse velocity and transverse position resolution.

REFERENCES

1. Atwood, W. B., Bowden, G. B., Bonneaud, G., Klem, D. E., Ogawa, A., Pestov, Yu. N., Pitthan, W. R. and Sugahara, R., Nucl. Instr. Meth., **206** (1983) 99.
2. G.V. Fedotovich, Yu.N. Pestov, and K.N.Putilin, *A Spark Counter with a Localized Discharge*, in: "Int. Conf. on Instrumentation for Colliding Beam Physics 1980", ed. Ann Mosher, Stanford Linear Accelerator Center, 1981.
3. Scotch® 57 electrical tape, 3M Co., Minneapolis, MN .
4. Stycast® HiK, Emerson & Cuming, Canton, MA 02021.
5. Model 2228A TDC, LeCroy Research Systems, NY. The 25 *ps/bin* conversion gain was obtained by modifying the unit.